

# Analysis of electronic parameters and interface states of boron dispersed triethanolamine/p-Si structure by AFM, $I$ - $V$ , $C$ - $V$ - $f$ and $G/\omega$ - $V$ - $f$ techniques

Fahrettin Yakuphanoglu <sup>a,\*</sup>, Salih Okur <sup>b</sup>

<sup>a</sup> Physics Department, Faculty of Arts and Sciences, Firat University, 23119 Elazig, Turkey

<sup>b</sup> Department of Physics, Faculty of Science, Izmir Institute of Technology, Gulbahce Campus, Urla, Izmir 35430, Turkey

## ARTICLE INFO

### Article history:

Received 16 March 2009

Received in revised form 27 April 2009

Accepted 13 May 2009

Available online 19 May 2009

### Keywords:

Metal/semiconductor contacts

Boron

Interfacial state density

## ABSTRACT

The electronic parameters and interface state properties of boron dispersed triethanolamine/p-Si structure have been investigated by atomic force microscopy,  $I$ - $V$ ,  $C$ - $V$ - $f$  and  $G/\omega$ - $V$ - $f$  techniques. The surface topography and phase image of the TEA-B film deposited onto p-Si substrate were analyzed by atomic force microscopy. The atomic force microscopy results show a homogenous distribution of boron particles in triethanolamine film. The electronic parameters (barrier height, ideality factor and average series resistance) obtained from  $I$ - $V$  characteristics of the diode are 0.81 eV, 2.07 and 5.04 k $\Omega$ , respectively. The interface state density of the diode was found to be  $2.54 \times 10^{10}$  eV<sup>-1</sup> cm<sup>-2</sup> under  $V_g = 0$ . The obtained  $D_{it}$  values obtained from  $C$ - $V$  and  $G/\omega$  measurements are in agreement with each other. The profile of series resistance dependent on voltage and frequency confirms the presence of interface states in boron dispersed triethanolamine/p-Si structure. It is evaluated that the boron dispersed triethanolamine controls the electronic parameters and interface properties of conventional Al/p-Si diode.

© 2009 Elsevier B.V. All rights reserved.

## 1. Introduction

Metal–semiconductor have been extensively investigated due to their technological applications. The electronic parameters of metal–semiconductor contacts can be modified by using organic materials and this modification could lead to an efficient barrier height and interface modification. Some studies have shown that the electronic parameters of the metal–inorganic diodes can be modified with various organic materials [1–12]. The control of metal/semiconductor diodes with organic materials is the key to fabricating reproducible metal/organic semiconductor/inorganic semiconductor rectifying devices. The new electrical properties of the metal–semiconductor contacts can be promoted by means of the choice of suitable material. We have believed that boron can modify the electronic properties of metal–semiconductor contacts by creation of physical barrier.

In the present study, for fabrication of Al/p-Si/TEA-B/Au, amorphous boron is dispersed in triethanolamine. Triethanolamine (TEA-C<sub>6</sub>H<sub>15</sub>NO<sub>3</sub>) is an organic chemical compound, which acts as a base due to the lone pair of electrons on the nitrogen atom over three hydroxyl groups. TEA is used as a pH balancer in cosmetic preparations in a variety of different products-ranging from skin

lotion, eye gels, moisturizers, shampoos, shaving foams etc. [13]. Triethanolamine (TEA) is also used as organic additive (0.1 wt.%) in the grinding of cement clinker, since it is proved to be very effective to prevent agglomeration and coating of the powder at the surface of balls and mill wall [14].

The electronic parameters and interface state density properties of Al/p-Si/TEA-B/Au diode have been investigated by using current–voltage characteristics and capacitance–conductance–voltage techniques.

## 2. Experimental

The organic/inorganic (Al/p-Si/TEA-B/Au) diode was prepared on a 530  $\mu$ m thick p-type single side polished silicon wafer with  $\langle 100 \rangle$  surface orientation and 2.0  $\Omega$  cm resistivity (purchased from Si-Mat Silicon Wafers Company, CZ). The wafer was chemically cleaned with the following procedure: The p-type Si wafer was dipped 10 min in boiling trichloroethylene, acetone and ethanol to remove organic contaminants. The natural SiO<sub>2</sub> layer on the Si wafer surface was removed by immersing in H<sub>2</sub>SO<sub>4</sub>, H<sub>2</sub>O<sub>2</sub> and 20%HF solutions, then 6HNO<sub>3</sub>:1HF:3.5H<sub>2</sub>O and 20%HF solutions. The wafer was rinsed thoroughly in de-ionized water with 18 M  $\Omega$  cm resistivity after each cleaning step. Then, low resistivity ohmic back contact to p-type Si wafer was made by using Al, followed by a temperature treatment at 570 °C for 5 min in N<sub>2</sub> atmosphere. Submicron size powdered amorphous boron (95–97 wt%

\* Corresponding author. Tel.: +90 424 2370000x6591; fax: +90 424 2330062.  
E-mail address: [fyhan@hotmail.com](mailto:fyhan@hotmail.com) (F. Yakuphanoglu).

a-B purity, Fluka, Switzerland) was dispersed in triethanolamine (TEA 99.5 wt% purity, Sigma–Aldrich) with 1 mg/ml concentration using a magnetic mixer at 50 °C about 4 h. The organic/inorganic TEA-B solution was spin coated on the cleaned *p*-type Si wafer with the 4500 rpm spin speed. The gold metal contacts with 200 nm thickness were thermally evaporated from a tungsten filament in  $5 \times 10^{-6}$  Torr using a mask with 2 mm diameter to form the top contact onto the (TEA-B)/*p*-Si film surface.

The TEA-B film on *p*-type Si was visualized with an atomic-force microscope (Solver P47H, NT-MTD) operating in the tapping mode on air in ambient conditions. A scanner, equipped with a scanning piezoelectric element (piezo scanner) with maximum scan range of  $10 \times 10 \times 2.5 \mu\text{m}$  has been used to obtain both surface morphology and phase images of the TEA-B films on *p*-Si substrate. A diamond like carbon (DLC) coated NSG01-DLC silicon cantilevers (NT-MTD) with a 2 nm tip apex curvature, a length of 130  $\mu\text{m}$ , a spring constant of 5.5 N/m, and resonance frequency of 150 kHz was used to take the topographies during the AFM scanning. The scan resolution was  $512 \times 512$  pixels. The images were processed by linear flattening method in order to remove the background slope, so the contrast and brightness were adjusted accordingly. The Nova 914 software package was used for controlling the SPM system and analyzing the AFM images.

The diode contact area was calculated to be  $3.14 \times 10^{-2} \text{ cm}^2$ . The current–voltage ( $I$ – $V$ ) characteristic of the Al/*p*-Si/TEA-B/Au diode was performed with 2400 KEITHLEY source meter and GPIB data transfer card for current–voltage measurements. The capacitance–conductance–voltage measurements were measured by using a 3532 HIOKI HITESTER LCR.

### 3. Results and discussion

#### 3.1. AFM results of the boron dispersed triethanolamine film on *p*-type silicon substrate

The AFM surface topography and phase images of the TEA-B film on *p*-Si substrate given in Fig. 1a and b, respectively, show a homogenous distribution of boron particles in TEA film. The root mean square (rms) surface roughness is obtained as 3.4 nm. The corresponding boron surface coverage was measured as 7%. The boron phase is clearly visible and easily separated from the TEA film in the AFM phase image.

#### 3.2. Current–voltage characteristics of Al/*p*-Si/TEA-B/Au diode

Fig. 2 shows the current–voltage characteristics of the Al/*p*-Si/TEA-B/Au diode. The diode indicates a rectifying behavior. The current–voltage characteristics of the Al/*p*-Si/TEA-B/Au diode can be analyzed by the following relation [15],

$$I = I_0 \exp\left(\frac{q(V - IR_s)}{nkT}\right) \left[1 - \exp\left(-\frac{q(V - IR_s)}{kT}\right)\right] \quad (1)$$

where  $R_s$  is the series resistance,  $V$  is the applied voltage,  $n$  is the ideality factor,  $k$  is the Boltzmann constant,  $T$  is the temperature and  $I_0$  is the reverse saturation current. The ideality factor of the diode was determined from the slope of the linear region of  $\log I$ – $V$  characteristics in forward bias and obtained  $n$  value is higher than unity. The higher value of ideality factor of the Al/*p*-Si/TEA-B/Au diode is attributed to the interface states and series resistance effects. These effects cause the non-ideal behavior. The effect of series

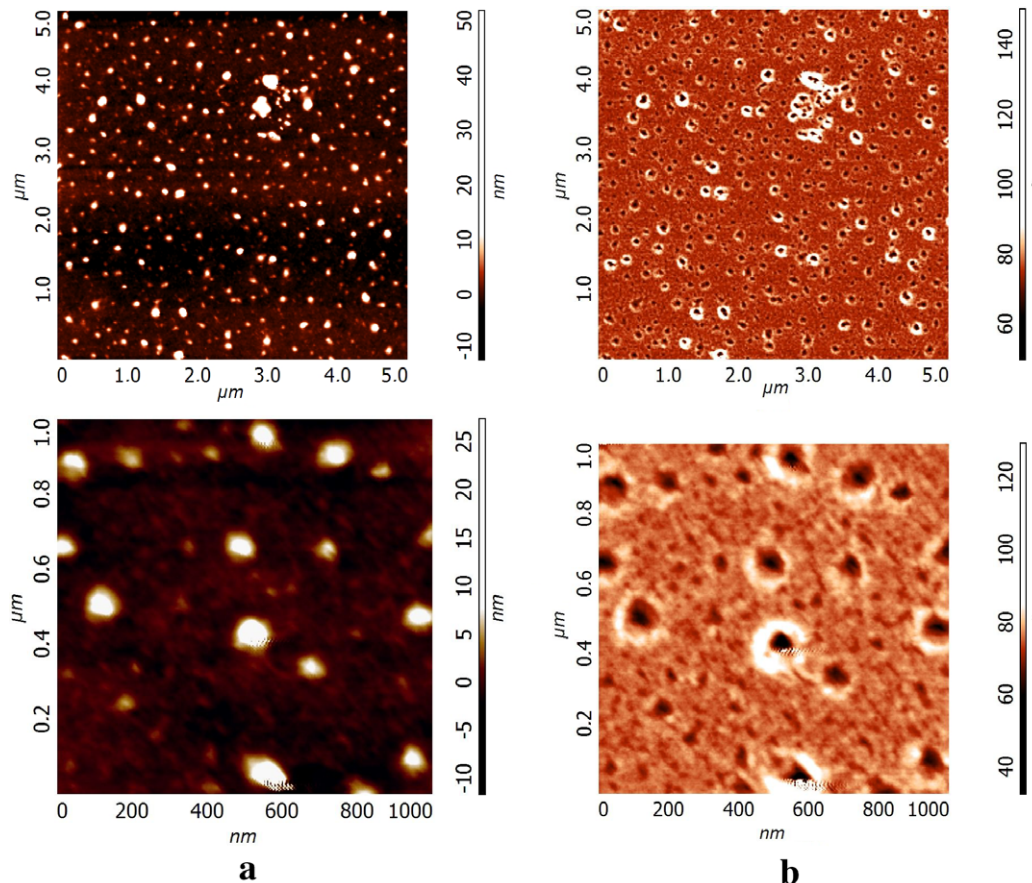


Fig. 1. (a) AFM topography and (b) phase image of the boron dispersed triethanolamine film on *p*-type silicon.

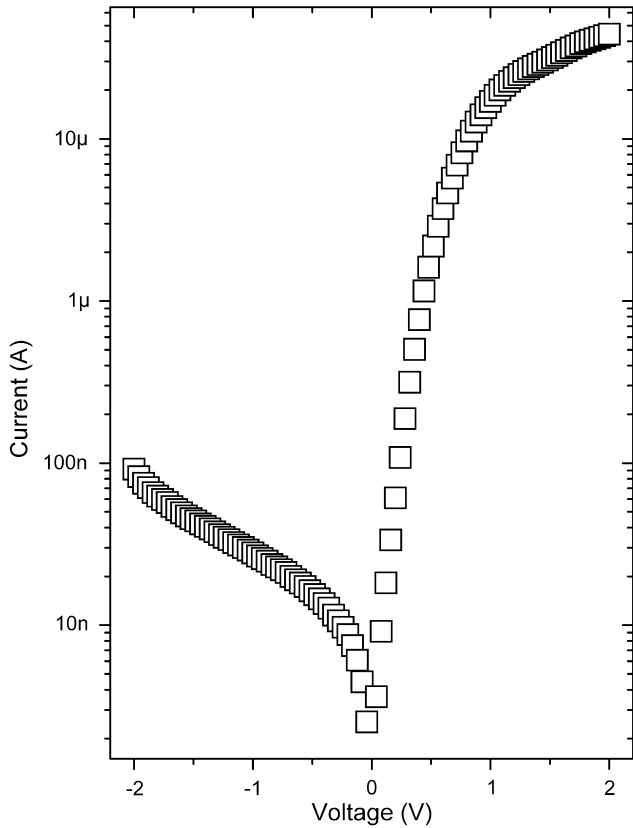


Fig. 2. Current–voltage characteristics of the Al/p-Si/TEA-B/Au diode.

resistance can be analyzed by Cheung’s method defined by the following relations [16],

$$\frac{dV}{d \ln(I)} = n \frac{kT}{q} + IR_s \quad (2)$$

and

$$H(I) = V - n \frac{kT}{q} \ln\left(\frac{I_0}{AA^*T^2}\right) = IR_s + n\phi_B \quad (3)$$

where  $\phi_B$  is the barrier height and  $q$  is the electronic charge. The plots of  $dV/d \ln I$  vs.  $I$  and  $H(I)$  vs.  $I$  are shown in Fig. 3. The  $R_s$  and  $n$  values were calculated from the slope and intercept of  $dV/d \ln I$  vs.  $I$  plot and were found to be 4.98 kΩ and 2.07, respectively. The  $R_s$  and  $\phi_B$  values were calculated from the intercept of  $H(I)$  vs.  $I$ .

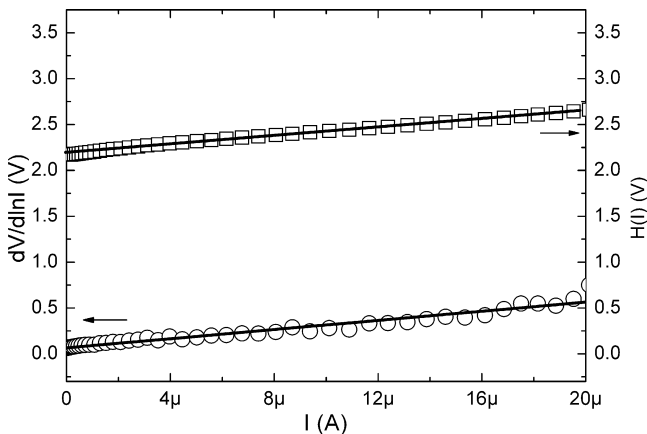


Fig. 3. Plots of  $dV/d \ln(I)$  vs  $I$  and  $H(I)$  vs  $I$  of the Al/p-Si/TEA-B/Au diode.

$I$  plot and were found to be 0.81 eV and 5.11 kΩ, respectively. The obtained ideality factor and barrier height values of the Al/p-Si/TEA-B/Au diode are higher than that of ideal metal/p-Si diode. This indicates that the boron dispersed triethanolamine interfacial layer modifies the barrier height of the diode by forming of a physical barrier between the metal and the Si inorganic wafer. The interface properties of the diode change with the boron dispersed triethanolamine layer and in turn, the electronic parameters of the diode are changed. The modification of semiconductor surfaces by boron dispersed triethanolamine leads to the changes in the interfacial properties of the diode, which cause the non ideal diode behavior.

### 3.3. Capacitance–voltage and interface state density properties of the Al/p-Si/TEA-B/Au diode

Fig. 4a and b shows the capacitance–voltage characteristics of the Al/p-Si/TEA-B/Au diode under various frequencies. The capacitance decreases with increasing frequency and reaches ideal MIS C–V curve for 1 MHz. As seen in Fig. 4b, the C–V curves under 5 kHz and 1 MHz confirm the metal–insulator layer–semiconductor structure (MIS) for the diode. The density per unit area of the charges in diode is calculated by the following relation [17],

$$Q_x = \left(\frac{C'_{ox}}{e}\right)(\phi_m - V_{FB}) \quad (4)$$

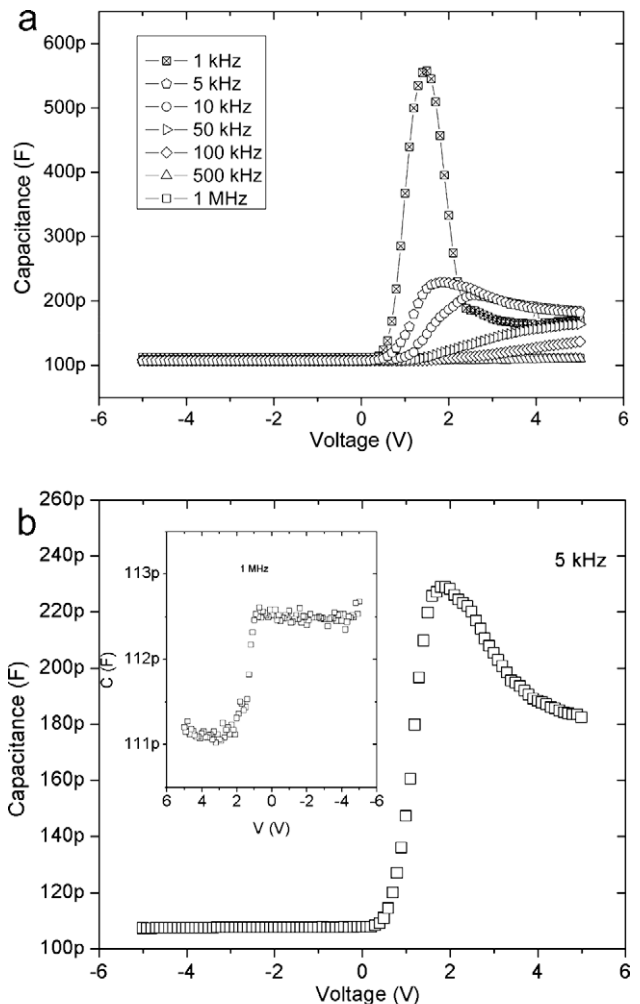


Fig. 4. Plots of C–V of the Al/p-Si/TEA-B/Au diode.

where  $C'_{ox}$  is the capacitance of the oxide layer per unit area,  $V_{FB}$  is the flat-band voltage,  $e$  is the electronic charge and  $\phi_m$  is the work function difference between silicon wafer and Al and whose value is  $-0.9$  V [18]. The flat-band voltage is an important parameter for assessing the quality of an MIS device. The  $V_{FB}$  and  $Q_x$  values for the diode were determined from the  $C-V$  characteristic of the diode under 5 kHz and were found to be  $-0.99$  V and  $9.97 \times 10^{13}$  Charges/m<sup>2</sup>, respectively. The negative value of the flat-band voltage is attributed to the contribution of the positive interface charges in the Al/p-Si/TEA-B/Au diode. The obtained  $Q_x$  value controls the conduction mechanism of the diode.

The density of interface states can be determined from  $C-V$  measurements by the following relation [19],

$$D_{it} = \frac{C'_{ox}}{q} \left( \left( \frac{d\Psi_s}{dV_g} \right)^{-1} - 1 \right) - \frac{C_{sc}(\Psi_s)}{q} \quad (5)$$

where  $C_{sc}$  is the capacitance of the semiconductor and  $\Psi_s$  is the surface band bending. The plot of  $D_{it}$  vs.  $V$  is shown in Fig. 5. The obtained  $D_{it}$  values are high and change with applied voltage. In order to check reliability of  $D_{it}$  values obtained, we use also the conductance method described by Nicollian and Brews [19]. In this technique, parallel capacitance  $C_p$  and conductance  $G_p$  expressions are defined as follows [19],

$$G_p = \frac{C_{it}}{2\tau} \ln(1 + \omega^2\tau^2) \quad (6)$$

and

$$C_p = C_d + \frac{C_{it}}{\omega\tau} \arctan(\omega\tau) \quad (7)$$

where  $C_{it} = qAD_{it}$ ,  $C_{it}$  is the interface state capacitance and  $A$  is the diode contact area,  $\omega$  is the angular frequency,  $\tau$  is the time constant of the interface states. To determine the interface state density for the diode, we plotted curves of  $(G/\omega)$  vs.  $\log f$  for the diode under various bias voltages, as shown in Fig. 6. As seen in Fig. 6, the plots of  $G/\omega-f$  indicate a peak. The origin of this peak is due to the presence of interface charges and these charges are present at interface of the silicon-oxide layer plus organic layer, which are contributing to the total charging current and in turn a peak appears in the  $G/\omega-f$  plot [20]. The peak position shifts with bias applied due to the distribution of the interface states. The interface state density of the diode was determined from Fig. 6 and was found to be  $2.54 \times 10^{10} \text{ eV}^{-1} \text{ cm}^{-2}$  under  $V_g = 0$ . The obtained  $D_{it}$  value is in agreement with  $D_{it}$  value obtained from  $C-V$  measurement. This indicates the consistency of both the methods.

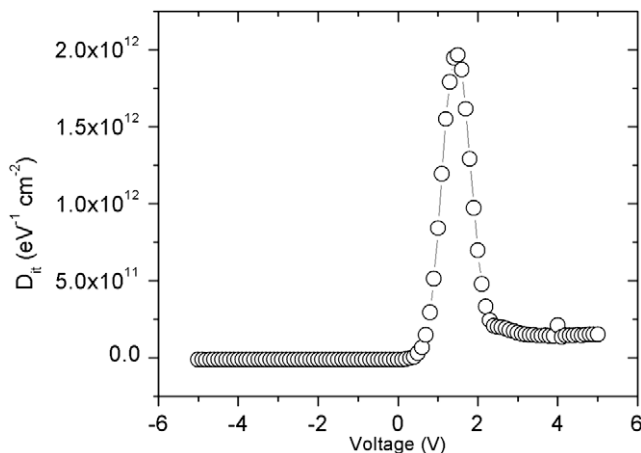


Fig. 5. Plots of  $D_{it}$  vs.  $V$  of the Al/p-Si/TEA-B/Au diode.

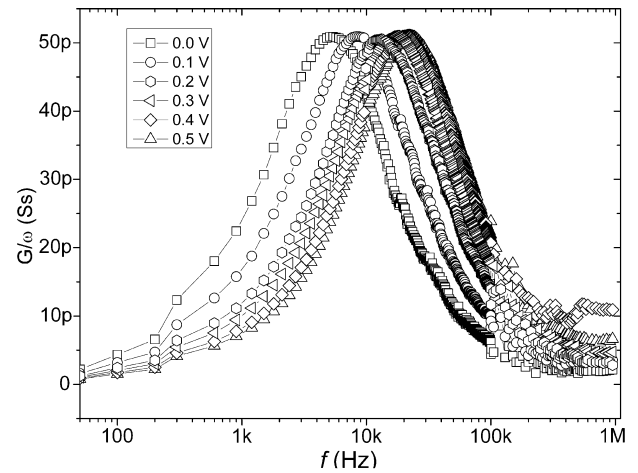


Fig. 6. Plots of  $G/\omega-f$  of the Al/p-Si/TEA-B/Au diode at various voltages.

Fig. 7 shows the capacitance–frequency plots of the diode under various bias voltages. The capacitance of the diode increases with decreasing frequency, because the interface states follow the alternating current–voltage (AC). At lower frequencies, the capacitance of the diode is dispersive, whereas at higher frequencies, the capacitance is non-dispersive because the charges at the interface states cannot follow the fast alternating current signal. Therefore, at low frequencies the total capacitance is equal to the sum of space-charge capacitance and interface capacitance, while at higher frequencies the total capacitance arises mostly from the space-charge capacitance [8,21].

Another important parameter for MIS devices is the series resistance. For the diode, the series resistance was directly measured by using a LCR meter and the series resistance plots under various voltages and frequencies are shown in Fig. 8a and b. As seen in Fig. 8a, the plots give a peak for various frequencies. The peak intensity decreases with the increasing frequency and the position of the peak shifts to higher voltages. The variation in the peak intensity indicates interface states following the alternating current. But, after 10 kHz, the peak disappears and this suggests that the interface states can not follow alternating current. As seen in Fig. 8b, at lower frequencies, the series resistance does not almost change with the frequency, whereas, at higher frequencies, it decreases and reaches a constant value. The profile of series resistance dependent on voltage and frequency is attributed to the particular distribution density of interface states.

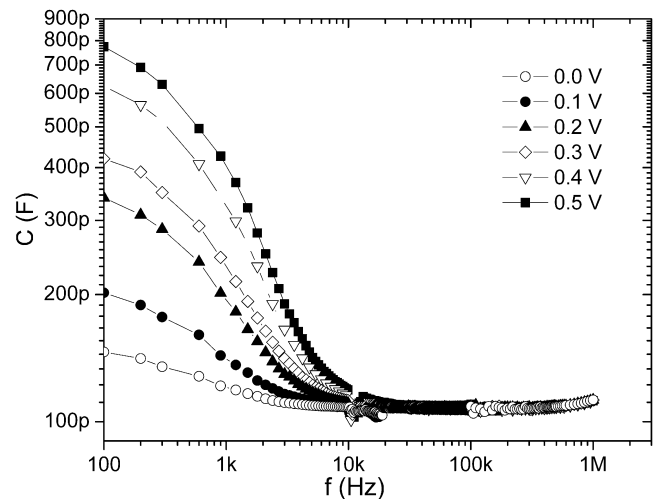


Fig. 7. Plots of  $C-f$  of the Al/p-Si/TEA-B/Au diode at various voltages.

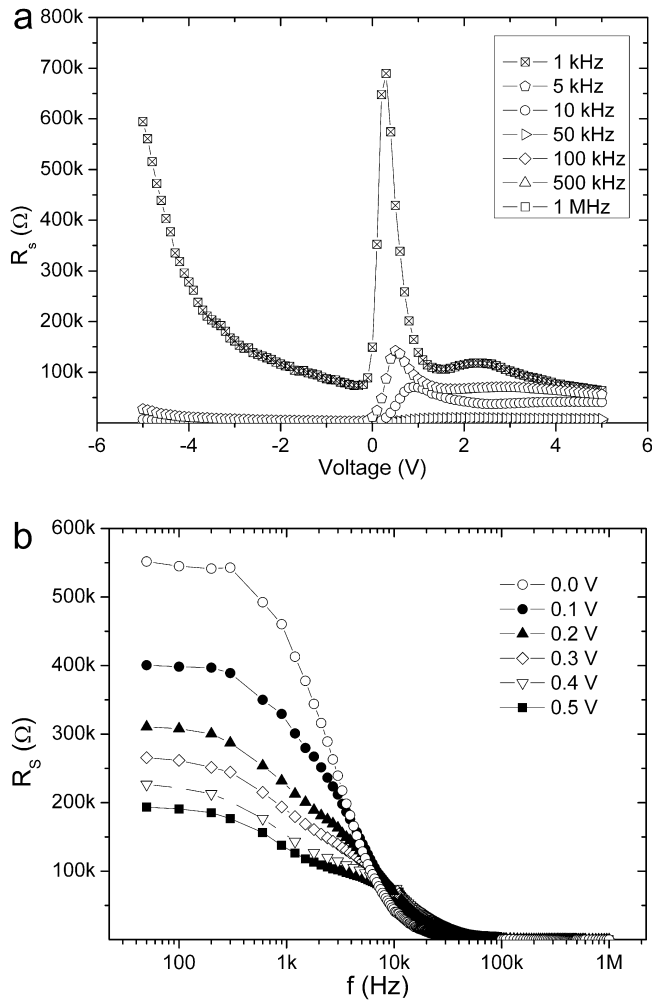


Fig. 8. Plots of  $R_s$ - $f$  of the Al/p-Si/TEA-B/Au diode at various voltages and frequencies.

#### 4. Conclusions

The boron dispersed triethanolamine/p-Si structure was fabricated and its electronic parameters and interface states were ana-

lyzed using  $I$ - $V$ ,  $C$ - $V$ - $f$  and  $G/\omega$ - $V$ - $f$  techniques. The surface topography and phase image of the TEA-B film deposited onto p-Si substrate were analyzed by atomic force microscopy. The barrier height, ideality factor, interface state density and average series resistance values of the diode were found to be 0.81 eV, 2.07,  $2.54 \times 10^{10} \text{ eV}^{-1} \text{ cm}^{-2}$  and  $5.04 \text{ k}\Omega$ , respectively. The electronic parameters and interface properties of conventional Al/p-Si diode are improved using boron dispersed triethanolamine thin film.

#### Acknowledgments

This work was supported by the National Boron Research Institute (BOREN) (Project No. BOREN-2006-26-Ç25-19) and by State Planning Organization of Turkey (Project No. DPT2003K120390). The authors wish to thank BOREN and the DPT.

#### References

- [1] I.H. Campbell, S. Rubin, T.A. Zawodzinski, J.D. Kress, R.L. Martin, D.L. Smith, *Review B* 54 (1996) 14321.
- [2] Ş. Aydoğan, M. Sağlam, A. Türüt, *Vacuum* 77 (2005) 269.
- [3] Ö. Vural, N. Yıldırım, Ş. Altındal, A. Türüt, *Synthetic Metals* 157 (2007) 679.
- [4] T. Kılıçoğlu, *Thin Solid Films* 516 (2008) 967.
- [5] Mehmet Enver Aydın, Fahrettin Yakuphanoglu, Jae-Hoon Eom, Do-Hoon Hwang, *Physica B* 387 (2007) 239.
- [6] M.A. Ebeoğlu, T. Kılıçoğlu, M.E. Aydın, *Physica B* 395 (2007) 93.
- [7] M.E. Aydın, F. Yakuphanoglu, *Journal of Physics and Chemistry of Solids* 68 (2007) 1770.
- [8] F. Yakuphanoglu, *Sensors and Actuators A* 141 (2008) 383.
- [9] Ş. Aydoğan, M. Sağlam, A. Türüt, *Microelectronic Engineering* 85 (2008) 278.
- [10] Ş. Karataş, C. Temirci, M. Çakar, A. Türüt, *Applied Surface Science* 252 (2006) 2209.
- [11] M.E. Aydın, F. Yakuphanoglu, T. Kılıçoğlu, *Synthetic Metals* 157 (2007) 1080.
- [12] M. Çakar, N. Yıldırım, H. Doğan, A. Türüt, *Applied Surface Science* 253 (2007) 3464.
- [13] Klaus Weissermel, Hans-Jürgen Arpe, Charlet R. Lindley, Stephen Hawkins, *Oxidation Products of Ethylene*, Industrial Organic Chemistry, Wiley-VCH, 2003, Chapter 7.
- [14] S. Sohoni, R. Sridhar, G. Mandal, *Powder Technology* 67 (1991) 277.
- [15] E.H. Rhoderick, R.H. Williams, *Metal-Semiconductor Contacts*, Clarendon, Oxford, 1988.
- [16] S.K. Cheung, N.W. Cheung, *Applied Physical Letters* 49 (1986) 85.
- [17] A. Donald, Neamen, *Semiconductor Physics and Devices-Basic Principles*, second ed., IrWin-McGraw-Hill, New York, 1997.
- [18] S.M. Sze, *Physics of Semiconductor Devices*, second ed., Wiley, New York, 1981.
- [19] E.H. Nicollian, J.R. Brews, *MOS (Metal Oxide Semiconductor)*, Physics and Technology, Wiley, New York, 1982.
- [20] M.E. Aydın, F. Yakuphanoglu, *Microelectronic Engineering* 85 (2008) 1836.
- [21] M. Çakar, Y. Onganer, A. Türüt, *Synthetic Metals* 126 (2002) 213.